Seasonal variations in viral distribution, dynamics and viral mediated host mortality in the Arabian Sea

Aparna Sreekumar, Parvathi Ammini, Jasna Vijayan, Pradeep Ram Angia Sriram, Sime-Ngando Telesphore

Seasonal variations in viral distribution, dynamics and viral mediated host mortality in the Arabian Sea

Aparna Sreekumar, Parvathi Ammini, Vijayan Jasna, Pradeep Ram, Télesphore Sime-Ngando

Seasonal variations in viral distribution, dynamics and viral mediated host mortality in the Arabian Sea.

Aparna S.[1], Parvathi A.[1*], Jasna V.[1,2], Pradeep Ram A. S.[3] and Sime-Ngando T.[3]

[1] CSIR-National Institute of Oceanography, Regional Centre (CSIR), Kochi-682 018, India

[2] Department of Aquatic Life Medicine, College of Fisheries Science, Pukyong National University, Busan, Republic of Korea

[3] Laboratoire Microorganismes : Génome et Environnement, UMR CNRS 6023, Université Clermont-Auvergne, 1 Impasse Amélie Murat, 63178 Aubière Cedex, France

∗ **Corresponding author**

Dr. Parvathi A

CSIR-National Institute of Oceanography

Regional Centre, Dr. Salim Ali Road,

Post Box No. 1913, Kochi-682 018, India

Ph: 91-(0) 484-2390814, Fax: 91-(0) 484-2390618

Email: parvathi@nio.org

Running page head: Seasonal variations in viral activities in the Arabian Sea

Abstract

Viruses are key players in the marine ecosystem. It is critical to study specific viral processes and their interrelationship with various biotic and abiotic variables to quantify their impact on the marine environment. This study investigates the influence of seasonality on viral distribution and their mediated processes in the coastal region of the southeastern Arabian Sea (India) for two consecutive years (2014 and 2015). Water samples were collected from four sampling stations, S1, S2, S3 and S4, in the southeastern Arabian Sea on a monthly basis. Samples were analyzed for the variations in viral abundance, viral production, and viral-induced host mortality covering three seasons namely, pre-monsoon, monsoon and post-monsoon. Viruses and bacteria were enumerated by epifluorescence microscopy following staining with SYBR Green I and viral production was estimated using viral dilution method. Seasonal variations in viral mediated mortality and microzooplankton grazing mortality of phytoplankton hosts were estimated by modified dilution method. The results revealed a pronounced seasonal pattern of viral abundance ($0.04\text{-}4.03 \times 10^7$ viruses mL^{-1}) and viral production ($0.71 \times 10^{10}\text{-}4.94 \times 10^{10}$ $L^{-1}d^{-1}$). The observed high viral-induced mortality of prokaryotes (25.85%) and phytoplankton (7.98–28.9%) during the pre-monsoon season was eventually linked to high viral abundance and production rates. Viral mediated processes were essentially linked to host density and water temperature. Transmission electron microscopy analysis revealed that myoviruses and non-tailed viruses were dominant in the study region with rod shaped bacteria being more susceptible to viral infection. The results indicated the prevalence of seasonally induced active viral processes in this tropical marine ecosystem which may significantly contribute to rapid recycling of nutrients in this region.

Keywords: Marine virus, viral induced prokaryotic mortality, viral production, viral morphotypes, nutrient recycling

Introduction

Viruses are the most numerous (10^{10} viruses per litre of seawater) and smallest biological entities in the marine environment which are capable of infecting almost all organisms. Viral mediated host lysis impacts marine biogeochemical cycles, host community composition, diversity and host evolution (Breitbart et al. 2018). Prokaryotes are the major hosts for marine viruses and phage numbers are highly correlated to prokaryote counts (Wommack and Colwell 2000; Jasna et al. 2017; Parvathi et al. 2018). Viral abundance is highly variable with respect to space and time. Short term to long term dynamics of viral abundance have been reported from different geographic locations (Rodriguez et al. 2000; Taylor et al. 2003; Clokie et al. 2006; Thomas et al. 2010; Parvathi et al. 2015; Jasna et al. 2017). Generally, viral abundance is highest in the euphotic zone and coastal environments compared to deeper waters and oligotrophic environments (Wommack and Colwell 2000; Parsons et al. 2012; Parvathi et al. 2018). However, subsurface peaks of viral abundance were observed in the mid latitude regions of the North Pacific (Yang et al. 2010). Studies also show that viral abundance and distribution are greatly influenced by the abundance and activities of their abundant hosts such as prokaryotes and phytoplankton (Taylor et al. 2003; Parsons et al. 2012; Gainer et al. 2017). Apart from prokaryotic abundance and chlorophyll *a* concentration, environmental variables like nutrients, temperature, salinity, sunlight, etc. are significant predictors of viral abundance in varying marine environments (Finke et al. 2017). Viral mediated mortality is also largely variable and have differential impacts on bacterial production in systems with different trophic status. Compared to grazer mediated mortality, viral mediated host mortality at times can dominate depending on the environment (Bettarel et al. 2004). Investigation across the North Atlantic Ocean reported viral mediated mortality as the major phytoplankton loss factor in the low and mid latitudes. Whereas, grazer mediated mortality dominated at higher latitudes (Mojica et al. 2016). Various studies have highlighted the importance of viral-mediated nutrient cycling over direct effect of viral-induced mortality, for promoting the growth of non-infected phytoplankton and bacterial populations (Weinbauer et al. 2011; Shelford et al. 2012).

The Arabian Sea has a unique hydrography influenced mainly by the seasonal reversal of monsoonal winds with high biological productivity. High primary productivity and existence of intense oxygen minimum zones (OMZ) and denitrification zones make the Arabian Sea a unique oceanic region (Naqvi et al. 1990; Olson et al. 1993; Gerson et al. 2014). During spring inter monsoon, the water column remains warmer and highly stratified with nutrient deficient surface waters, whereas, wind driven coastal upwelling during southwest monsoon and convective

85 overturning of surface waters due to winter cooling in the northeast monsoon render the water column well mixed
86 during both the monsoons (Prasanna Kumar and Prasad 1996; Gerson et al. 2014). Several studies have reported
87 seasonal variations in bacterial abundance and primary productivity associated with physical forcing in the Arabian
88 Sea (Campbell et al. 1998; Ramaiah et al. 2009). High primary productivity during the southwest monsoon was
89 found to be associated with high nutrient availability (Prasanna Kumar et al. 2000). The physical forcing in the
90 Arabian Sea arising from a unique combination of climate, wind, and circulation imparts seasonal variations in
91 trophic conditions and brings in huge diversity (Burkhill et al. 1993; Mantoura et al. 1993). Some of the
92 investigations conducted in the Arabian Sea concluded a close coupling of bacterial production with primary
93 production during summer and winter monsoons (Wiebinga et al. 1997). During high primary production, the labile
94 (rapidly degradable) dissolved organic carbon (DOC) produced by phytoplankton are rapidly used by the bacteria (in
95 hours or days). In contrast, at time of low primary production, high bacterial abundance and production may be
96 sustained by semi-labile DOC that can last from weeks to months in the water column (Calleja et al. 2019). Thus, at
97 both times (during high and low primary production) the DOC pool is sustaining bacterial growth. High bacterial
98 abundance and production at time of low primary production, especially during the spring and fall inter monsoons
99 suggests of predominance of microbial loop in the sustenance of the dissolved organic carbon (DOC) pool (Ducklow
100 1993; Ramaiah et al. 1996; Campbell et al. 1998). A recent report by Sabbagh et al. (2020) suggests that
101 heterotrophic bacteria are controlled by viruses most of the year in the coastal waters of the Red sea. This indicates
102 that viral-induced mortality is one of the major regulators that control bacterioplankton standing stocks.
103 To date, few reports are available on viruses in the Arabian Sea (Brum et al. 2013; Jain et al. 2014; Parvathi et
104 al. 2018). Parvathi et al. (2018) have studied the viral abundance, viral processes and viral life strategies in the
105 oxygen minimum zones of the Arabian Sea. The morphological diversity of the viruses and their characteristic
106 features were examined as a part of TARA Ocean expedition (Brum et al. 2013). Jain et al. (2014) reports on the
107 seasonal variations in viral abundance and virus-to prokaryote ratio. However, no information exists on the seasonal
108 variations in viral processes in the Arabian Sea to date. To better understand the impact of viruses in the marine
109 environment, it is critical to study specific viral processes and their interrelationship with various biotic and abiotic
110 variables. Moreover, estimation of parameters like viral production, turnover rates, and viral mediated mortality are
111 essential for the incorporation of viral processes into various ecosystem models. Recent studies by Jasna et al. (2017,
112 2019) from an estuarine region (Cochin estuary) in the southwest coast of India reports on the seasonal variations in

viral abundance, viral production and viral process. These studies reveal that distinct seasons such as monsoon, pre- and post-monsoons have profound influence on viral abundance and production. The present study is one among the few in the Arabian Sea, specifically the southeastern Arabian Sea, to investigate the seasonality in viral distribution and viral processes. We hypothesize that there could be a significant seasonal variation in the viral distribution and viral mediated mortality in the study region and viral lysis may play a significant role in the microbial loop in this part of the southeastern Arabian Sea.

Materials and methods

Sampling locations, physical and chemical parameters

Water samples were collected from four sampling stations, S1, S2, S3 and S4, located in a transect perpendicular to the coast of Kochi (south west coast of India), in the eastern Arabian Sea (Fig 1). Station S1, has a depth of ~30 m whereas, S2, S3, and S5 have a depth of 22 m, 14 m and 6 m, respectively. Samples were collected during three distinct seasons namely, pre-monsoon (PRM), monsoon (M) and post-monsoon (PM) from three depths (surface, middle and bottom) of S1 (0.5 m, 15 m and 30 m), S2 (0.5 m, 11 m, and 22 m), and S3 (0.5 m, 7 m, and 14 m), and from two depths of S4 (0.5 m and 6 m) on a monthly basis for two consecutive years, 2014 and 2015. Totally 253 samples were collected from all the four stations in the study. In June 2014 (M), sampling was not done due to adverse climatic conditions. Water samples were collected using a 5L Niskin sampler (Hydro-Bios, Germany). Samples were transferred to acid washed sterile glass bottles and were transported to the laboratory in an ice box maintained at 4°C. Vertical profiles of temperature and salinity were recorded using a conductivity temperature density (CTD) profiler (SBE Seabird 19, Sea-Bird Scientific, Bellevue, WA, USA) with accuracy ± 0.001°C and ± 0.001 S/m for temperature and conductivity, respectively. Samples for dissolved oxygen (DO) were withdrawn from the niskin sampler into DO bottles (60 mL) without trapping air bubbles, allowing the bottles to overflow with at least one liter to avoid exchange with atmospheric oxygen. The dissolved oxygen in the bottle was fixed with 0.5 mL each of Winkler reagents and estimated by Winkler's titration method (Grasshoff 1983). Inorganic nutrients such as nitrate, nitrite and phosphate present in the water samples were estimated by spectrophotometric analysis (Grasshoff 1983). To determine the Chl *a*, samples were first filtered through 0.7 µm GF/F (Whatman, USA), treated with 90% acetone overnight in dark at 4°C, and the pigment was measured fluorometrically (Parsons et al. 1984).

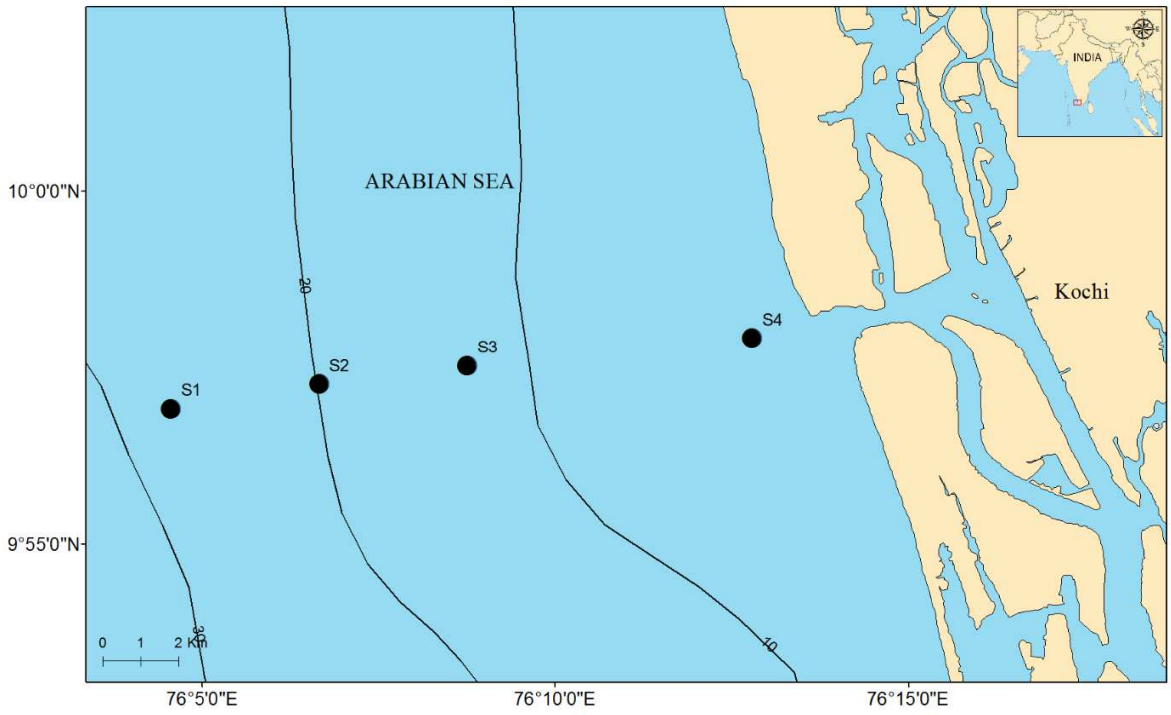

Fig. 1 Sampling locations in the Arabian Sea. Water samples were collected from four stations of a transect perpendicular to the coast of Kochi on monthly basis during 2014 and 2015. Sampling locations are marked as S1, S2, S3 and S4

Abundance of viruses and prokaryotes

Viruses and bacteria in the sample were enumerated by epifluorescence microscopy following the SYBR Green I staining method (Patel et al. 2007). Immediately after collection, 1 mL each of the samples were fixed with formalin (37% (*w/v*) formaldehyde, 0.02 µm filtered) to a final concentration of 2% (*v/v*). The samples were then kept on ice for 10 min in dark and subsequently filtered (< 20 KPa vacuum) through 0.02 µm Anodisc filters (Whatman). The filters were dried completely and stained with 100 µL each of 1:40 diluted SYBR Green I commercial stock for 20 min. Excess stain was removed and the filters were mounted on glass slides with 30 µL of 0.1% (*v/v*) anti-fade mounting medium (*p*-phenylenediamine). The slides were observed under an epifluorescence microscope (Olympus BX 41, Olympus, USA) for the enumeration of viruses and prokaryotes. Prokaryotes and viruses could be distinguished from each other based on their relative sizes. Viruses appeared as numerous green pinpricks, whereas,

bacteria were larger and possessed definite shapes. A blank was routinely examined as a control for contamination of equipment and reagents.

Viral Production and turnover rates

Viral production rates in the surface water samples of stations S1 and S4 during the three seasons (pre monsoon, PRM; monsoon, M; post monsoon, PM) in the year 2014 were estimated by diluting the water sample (100 mL) in triplicates with three volumes of ultra-filtered (using CDUF001LT, Millipore, USA, with a membrane having molecular weight cut-off or MWCO of 100 kDa) virus-free seawater and subsequently incubating them at room temperature (30°C) in the dark for 24 h. Subsamples (1 mL) were collected every 3 h to enumerate viruses and prokaryotes (Wilhelm et al. 2002). Viral production rates were estimated from the first order regression of increase in viral abundance over time, after correcting for the dilution of prokaryotes in the experimental sample, using the formula, Viral production, VP = m × (P/p), where 'm' is the slope of the regression line, 'p' is the concentration of prokaryotes after dilution, and 'P' is the concentration of prokaryotes prior to dilution. Viral turnover rates (VTR) were estimated from the ratio of viral production to viral abundance in the undiluted sample.

Viral induced prokaryotic mortality (VIPM) and phenotypic diversity of viruses

In order to determine the prokaryotic mortality due to viral lysis, surface water samples from S1 and S4 during the three seasons (PRM, M and PM) were collected and fixed with formalin (final concentration of 2% v/v). Prokaryotic cells in the sample were gathered on a 400-mesh formvar grid by ultracentrifugation (Beckman Coultor SW40 Ti Swing-Out-Rotor, 70,000 × g, 20 min at 4°C). The grids were stained with uranyl actate (2% w/w) for 30 s and washed twice with 0.02-µm filtered distilled water and dried completely (Pradeep Ram et al. 2010). The stained grids were observed using a JEOL 1200EX transmission electron microscope (20,000-60,000 X magnification). Frequency of visibly infected cells (FVIC) were determined by examining 600-800 prokaryotic cells per grid. A minimum of 15 infected cells were examined to determine the average burst size (BS). Frequency of infected cells (FIC) and viral induced prokaryotic mortality (VIPM) were estimated using the following formulae: $FIC = 9.524\ FVIC - 3.256$ (Weinbauer et al. 2002) and $VIPM = (FIC + 0.6 \times FIC^2)/(1 - 1.2 \times FIC)$ (Binder 1999). During the transmission electron microscopy analysis, visualization of viruses was performed at a magnification of 65,000-1,00,000. Viruses were classified as myoviruses, podoviruses, siphovirues, and non-tailed viruses based on their morphology (Borrel et al. 2012)

178 **Viral mediated mortality (VMM) and microzooplankton grazing mortality (MGM) of phytoplankton hosts**

179 Seasonal variations in viral mediated mortality (VMM) and microzooplankton grazing mortality (MGM) of
180 phytoplankton hosts in the surface waters of S1 and S4 were estimated by modified dilution method (Evans et al.
181 2003). Samples were collected during the three seasons: PRM, M and PM. Two parallel dilution series (20%, 40%,
182 70% and 100%) of the whole seawater, one with grazer-free diluent (0.2-µm filtered) and the other with virus-free
183 diluent (100 kDa filtered), were prepared after removing the mesoplankton size fraction through a 200 µm nylon
184 mesh (1L final volume). The bottles were incubated under *in situ* conditions of temperature (28-30 °C) and light for
185 a period of 24 h. Subsamples were collected at 0 h and 24 h for the enumeration of phytoplankton host populations.
186 Apparent growth rate (k, d^{-1}) of phytoplankton in each bottle were calculated using the equation,

187 $$k = \ln({}^{P_t}/_{P_0})/t$$

188 where 'P_0' and 'P_t', respectively, are the plankton abundance before and after incubation and 't' is the time interval
189 for the incubation.

190 A first order regression of apparent growth rate against fraction of seawater (for both 0.2 µm and 100 kDa) was
191 used for the estimation of mortality due to gazing (m_g) and combined mortality due to grazing and viral lysis (m_{g+v})
192 for those incubations that produced significantly different regression slopes for the two dilution series as determined
193 from an F-test. Regression coefficients of the 0.2 µm series and the 100 kDa series represent the microzooplanton
194 grazing rates (m_g) and the combined mortality rates of microzooplankton grazing and viral lysis (m_{g+v}), respectively
195 (Evans et al. 2003; Ortmann et al. 2011; Cram et al. 2016). Viral mediated mortality (m_v) can be estimated using the
196 formula,

197 $$m_v = m_{g+v} - m_g$$

198 Percentage of viral mediated mortality and microzooplankton grazing mortality were estimated using the
199 equations,

200 $$\%\, VMM = (1 - e^{-m_v}) \times 100$$

201 $$\%\, MGM = (1 - e^{-m_g}) \times 100$$

202 **Statistical analysis**

203 Potential relationship among different biological, physical and chemical variables were tested by Pearson correlation
204 analysis. Principal component analysis (PCA) using PAST software version 3 (Hammer et al. 2001) was also

employed for analyzing the major variables influencing viral abundance and dynamics during the three distinct seasons. To discern the biotic and abiotic predictor variables which drive the seasonal variations in viral abundance, a distance based linear modeling analysis (distLM) was performed using Primer 7 software (McArdle and Anderson 2001). Significant inter-annual, seasonal and spatial variability in different biotic and abiotic variables were tested by three-way ANOVA using the trial version of SPSS software.

Results

Spatial and vertical variability in physical and chemical parameters

Temperature varied vertically along the water column. Surface waters had an average temperature of 29.25 ± 1.34°C in 2014 and 29.25 ± 1.87°C in 2015 (Average values of all stations combined). Middle and bottom waters were cooler than surface waters. In all the three seasons, highest temperature was recorded in the surface waters at all the four stations (Online Resource 3). DO exhibited significant spatial variability ($p < 0.001$) and varied between depths in all the stations with the surface having the highest value compared to middle and bottom (Tables 2 & 3). The lowest values of DO were estimated from the bottom waters of all the stations during M except for station 4 in 2014 which had the highest DO concentration in bottom waters during monsoon (7.11 mL L^{-1}). Salinity of the four stations varied significantly ($p < 0.001$) with the offshore stations (S1 and S2) having higher salinities when compared to near-shore stations (S3 and S4). The average salinity at S1 was recorded as 34 ± 2.45 in 2014 and 34.02 ± 1.26 in 2015. Whereas, at S4, the salinity was 30.8 ± 0.74 and 32.7 ± 2.4 in the years 2014 and 2015, respectively. The salinity of near-shore stations was influenced by the freshwater input from the Cochin estuary with maximum influx during south west monsoon and least during PRM periods. The seasonal values of salinity varied significantly ($p < 0.05$) between the two years. Chl *a* also exhibited significant spatial variations ($p < 0.001$) with highest concentrations at the near-shore stations as compared to offshore stations (Tables 2& 3). Concentrations of dissolved inorganic nutrients like NO_3 and PO_4 were higher in bottom waters as compared to surface waters (Tables 2& 3). NO_3 concentration of the water column ranged from 0.05-24.47 µmol L^{-1} in 2014 and 0.1-22.41 µmol L^{-1} in 2015. Nitrogen to Phosphorous (NP) ratio of the study region ranged from 0.33-18.21 in 2014 and 0.52-19.67 in 2015.

Seasonal variability in physical and chemical parameters

Each year was divided into three seasons, PRM, M and PM for comparison. Seasonal variations were prominent for most of the parameters studied. In both the years, temperature was maximum during PRM (29.81 ± 0.8°C in 2014

and 30.14 ± 0.72°C in 2015), followed by PM (28.93 ± 0.6°C in 2014 and 28.67 ± 0.44°C in 2015) and the lowest during M (26.41 ± 1.59°C in 2014 and 24.98 ± 1.13°C in 2015) (Online Resource 1). Salinity was highest during PRM and averaged 33.95 ± 1.09 in 2014 and 33.62 ± 1.96 in 2015 (Online Resource 1). The lowest salinity was observed during M with average values of 30.23 ± 1.76 in 2014 and 29.98 ± 2.11 in 2015. However, the seasonal variations in salinity was not significant statistically. Dissolved oxygen (DO) concentrations exhibited significant seasonal variability ($p < 0.001$) (Table 1). The PM season had the highest DO concentrations (6.19 ± 1.87 mL L^{-1} in 2014 and 7.89 ± 1.54 mL L^{-1} in 2015), whereas, PRM was estimated to have the lowest DO in both the years (4.82 ± 1.48 mL L^{-1} in 2014 and 4.83 ± 2.97 mL L^{-1} in 2015). Concentrations of nutrients like NO_3, SiO_4 and PO_4 had significant seasonal variations ($p < 0.001$) with highest values during M and the least during PRM. NO_3 concentration in the water column ranged 0.45-24.47 µmol L^{-1} (in 2014) and 0.17-22.41 µmol L^{-1} (in 2015) during M and 0.05-2.42 µmol L^{-1} (in 2014) and 0.30-3.97 µmol L^{-1} (in 2015) during PRM. Chl *a* concentration was significantly high during M (4.45 ± 0.8 mg m^{-3}) and low during the other two seasons (0.68 ± 0.74 mg $m^{-3}$and 0.61 ± 0.50 mg m^{-3} during PRM and PM, respectively) (Online Resource 1). The Chl *a* concentration increased by 2 to 5-fold from PRM to M (Online Resource 1). At the nearshore stations, Chl *a* was comparatively high during all the seasons indicating the influence of nutrient input from the estuary.

Inter-annual variability in physical and chemical parameters

The average values (calculated for each depth of the four stations) of physical, chemical and biological-variables in the three seasons of the two years are listed in Tables 2 and 3. Dissolved oxygen, NH_4, SiO_4 and PO_4 showed significant inter-annual variations ($p < 0.001$) (Table 1). DO concentrations (of all depths and stations) ranged from 0.21-11.90 mL L^{-1} in 2014, and 0.58-10.92 mL L^{-1} in 2015 in the study area. The average dissolved inorganic nutrient concentration (of all depths and stations) was highest in 2014 (NH_4, 5.58 ± 7.81 µmol L^{-1}; PO_4, 0.86 ± 0.84 µmol L^{-1}; SiO_4, 11.76 ± 8.49 µmol L^{-1}) as compared to 2015 (NH_4, 3.20 ± 2.88 µmol L^{-1}; PO_4, 0.40 ± 0.38 µmol L^{-1}; SiO_4, 8.74 ± 9.05 µmol L^{-1}). Temperature, salinity and Chl *a* exhibited no significant inter-annual variations. Temperature ranged from 23.05-31.57°C in 2014 and 23.09-31.87°C in 2015 (of all depths and stations). Seasonal variation in temperature between the two years was prominent in the study area ($p < 0.05$). The average salinity was 33.08 ± 3.75 in 2014 and 33.56 ± 1.89 in 2015 (Average value of all depths, and stations). Chl *a* concentration in the study region ranged 0.03-30.60 mg m^{-3} in 2014 and 0.01-30.60 mg m^{-3} in 2015.

Variations in viral and prokaryotic abundance

Seasonal variations in viral and prokaryotic abundances were significant in all the stations with PRM having the highest abundance followed by PM and M (Fig 2). Viral abundance (VA) (represented as viral like particles or VLPs) showed significant ($p < 0.001$) inter-annual variations (Table 1) ranging from 0.07-2.08 $\times 10^7$ VLP mL^{-1} in 2014 and 0.04-4.03 $\times 10^7$ VLPs mL^{-1} in 2015 (values from all depths and stations). Viral and prokaryotic abundances varied significantly among stations ($p < 0.05$ and $p < 0.001$, respectively). The average VA (all depths combined for each station) was significantly greater at the near-shore stations ($0.46 \pm 0.37 \times 10^7$ VLPs mL^{-1} in 2014 and $0.72 \pm 0.8 \times 10^7$ VLPs mL^{-1} in 2015) as compared to the offshore stations ($0.34 \pm 0.22 \times 10^7$ VLPs mL^{-1} in 2014 and $0.74 \pm 0.63 \times 10^7$ VLPs mL^{-1} in 2015). In general, highest abundances were estimated in the surface waters followed by middle and bottom waters (Tables 2 & 3). However, there was no statistically significant variations in VA between these three depths. Prokaryotic abundance (PA) ranged from 0.17-3.3 $\times 10^6$ cells mL^{-1} during 2014 and 0.01-4.71$\times 10^6$ cells mL^{-1} during 2015. Although there was a similar vertical pattern of PA as that of VA, the variations were not statistically significant. PA also exhibited seasonal and spatial variations (Tables 2 & 3). VA was positively correlated to PA ($p < 0.001$) and Chl *a* ($p < 0.005$), whereas, PA showed significant positive correlations with temperature ($p < 0.001$) and DO ($p < 0.001$).

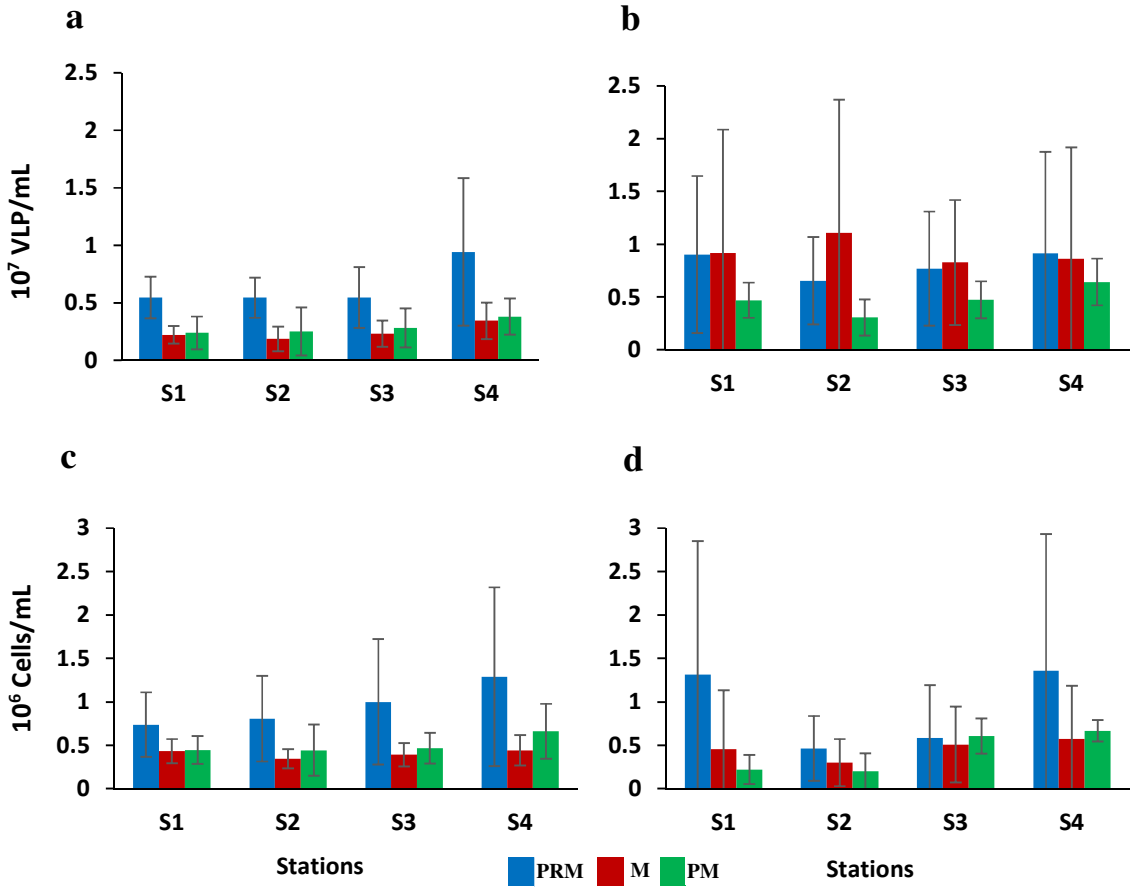

Fig. 2 Variations in viral and prokaryotic abundance (VA & PA) during pre-monsoon (PRM, blue), monsoon (M, red) and post monsoon (PM, green) seasons. (a) VA in 2014, (b) VA in 2015, (c) PA in 2014 and (d) PA in 2015

Viral production (VP) and viral turnover rates (VTR) in surface waters

VP and VTR from surface waters during the three seasons of 2014 are presented in Fig. 3. Viral production rates were higher during PRM ($4.48 \pm 0.83 \times 10^{10}$ $L^{-1}d^{-1}$ at S1 and $4.94 \pm 1.6 \times 10^{10}$ $L^{-1}d^{-1}$ at S4), followed by PM ($1.93 \pm 0.86 \times 10^{10}$ $L^{-1}d^{-1}$ at S1 and $3.16 \pm 0.63 \times 10^{10}$ $L^{-1}d^{-1}$ at S4) and lowest during M ($0.71 \pm 0.63 \times 10^{10}$ $L^{-1}d^{-1}$ at S1 and $1.45 \pm 0.87 \times 10^{10}$ $L^{-1}d^{-1}$ at S4). Viral turnover rates (VTR) ranged from 9.04-46.39 d^{-1} and followed the same pattern as VP except that S1 had the highest turnover rates compared to S4.

283

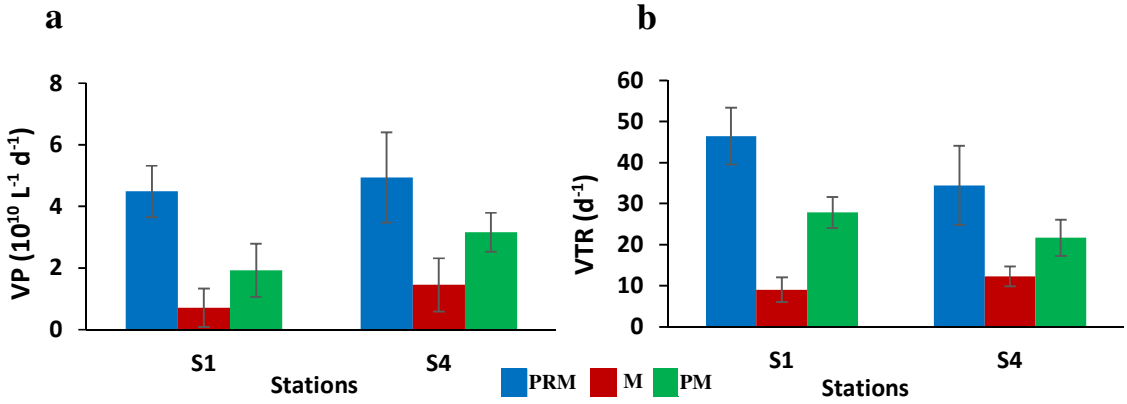

Fig. 3. Variations in (a) viral production (VP) and (b) viral turnover rates (VTR) at stations S1 and S4 during pre-monsoon(PRM, blue), monsoon (M, red) and post monsoon (PM, green) in 2014

284 **Viral induced prokaryotic mortality (VIPM) as determined by TEM analysis**

285 FIC averaged 17.7 ± 2.33%, 7.3 ± 1.86% and 10.79 ± 2.87% for PRM, M and PM, respectively (Fig. 4). VIPM,
286 which was estimated from FIC and it ranged from 5.86-28.64% with an average of 13.63 ± 7.19%. The annual
287 average of VIPM at S1 and S4 were 15.16 ± 6.63% and 12.09 ± 7.75%, respectively. PRM was marked with the
288 highest VIPM (24.15 ± 6.35% at S1 and 25.85 ± 3.95% at S4) compared to other seasons (Fig. 4).

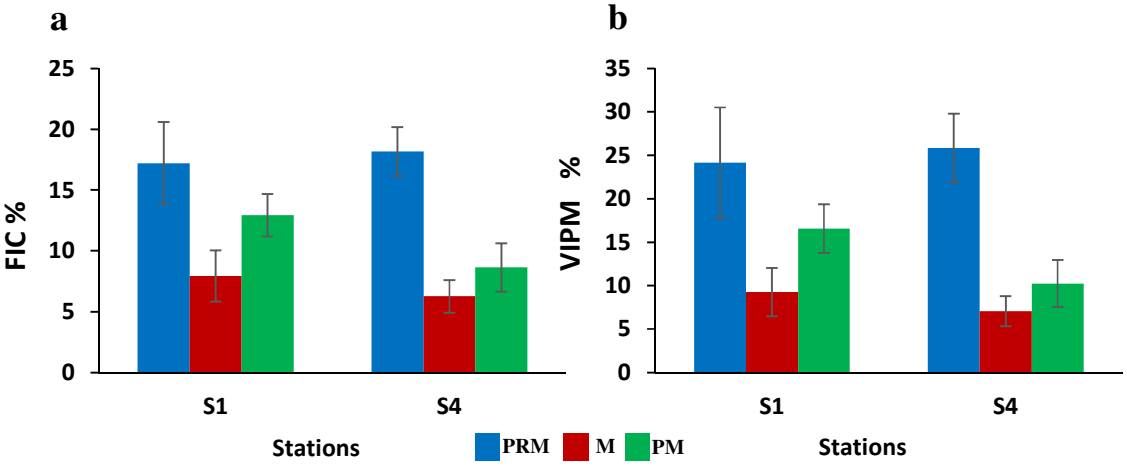

Fig. 4 Seasonal variations in (a) frequency of infected cells (FIC) and (b) viral induced prokaryotic mortality (VIPM) at S1 and S4 in 2014. Pre-monsoon(PRM): blue; monsoon (M): red; post monsoon (PM): green

289

290 **Viral mediated mortality (VMM) of phytoplankton by the modified dilution method**

291 The modified dilution experiment was carried out to estimate the viral mediated mortality (VMM) and
292 microzooplankton grazing mortality (MGM) of phytoplankton during PRM, M and PM in 2014 for water samples
293 collected from S1 and S4 (Fig. 5). VMM was greater during PRM (28.9 ± 11.35% and 26.24% at S1 and S4,
294 respectively), followed by PM (10.78 ± 12.71% at S1 and 13.7 ± 6.67% at S4). Lowest mortality was observed
295 during M (7.98 ± 2.65% and 9.83 ± 1.36% at S1 and S4, respectively). MGM followed the same pattern at S1 (14.91
296 ± 4.97%, 6.47 ± 0.65% and 10.21 ± 5.4% during PRM, M and PM, respectively). However, at S4, MGM was greater
297 during PM (19.12 ± 3.82%), followed by PRM (15.21 ± 9.56%) and M (10.9 ± 0.47%). VMM was greater compared
298 to MGM at both stations during PRM and M.

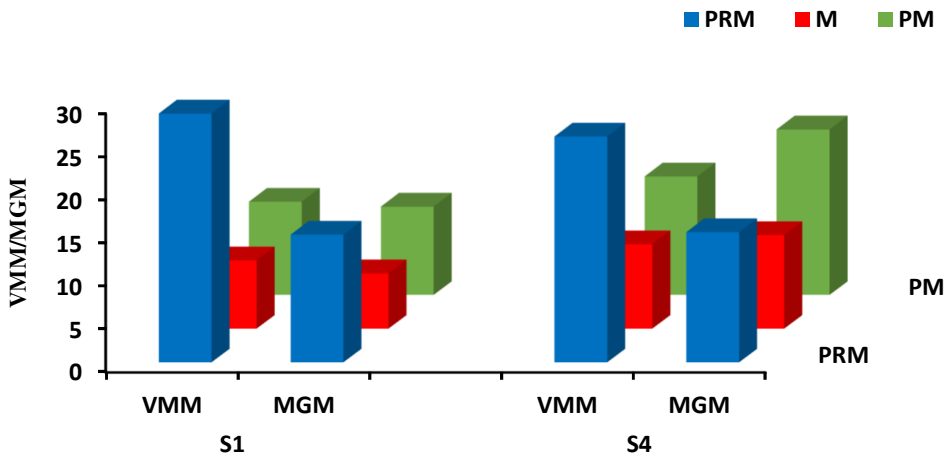

Fig. 5 Seasonal variations in viral mediated mortality (VMM) and microzooplankton grazing mortality (MGM) at S1 and S4 in 2014. pre monsoon (PRM): blue; monsoon (M): red; post monsoon (PM): green

307

308 **Seasonal variations in viral morphotypes and virally infected prokaryotic morphotypes**

309 TEM analysis of viruses from the study area revealed the dominance of four morphotypes: myoviruses (long
310 contractile tails), siphoviruses (long non-contractile tails), podoviruses (short non-contractile tails) and non-tailed
311 viruses (Fig. 6). Myoviruses were dominant during PRM and PM seasons (48% and 40%, respectively), whereas,
312 non-tailed viruses were the major group during M (38%) (Fig. 7). Non-tailed viruses were the second major group
313 after myoviruses forming 22%, 38% and 28% during PRM, M and PM seasons, respectively. Siphoviruses and
314 podoviruses represented the next most abundant morphotypes.

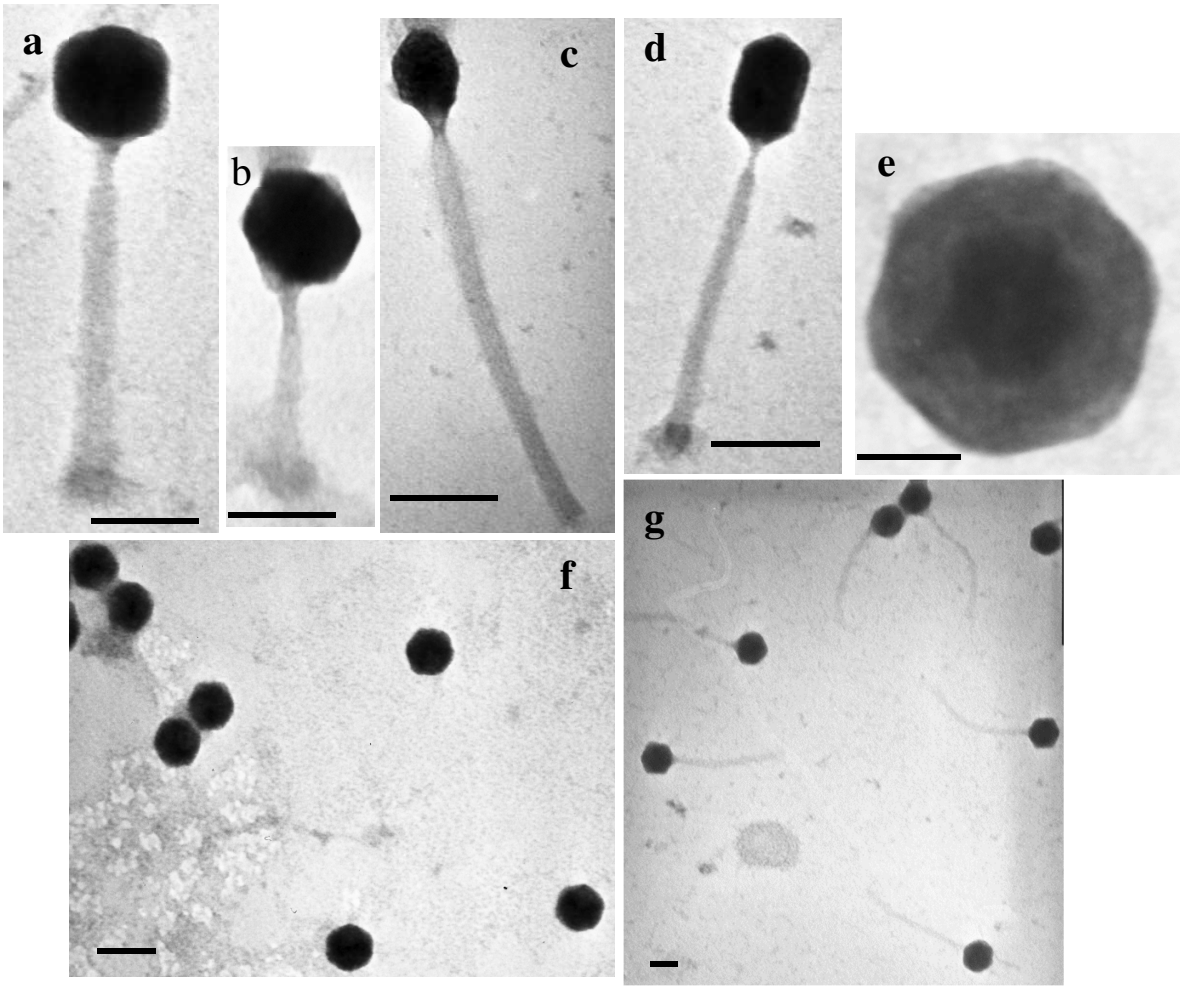

Fig. 6 Viral morphotypes from the Arabian Sea (a, b, c, d) myoviruses, (e, f) non-tailed viruses and (g) siphoviruses. Scale bar = 50 nm

The prokaryotic morphotypes as revealed by TEM analysis belonged to five groups, short rods, elongated rods, fat rods, cocci and filamentous rods (Fig. 8). Overall, the rods represented the major fraction of virally infected cells in the study region. Among rods, elongated rods were the most infected ones during PRM (32%), followed by short rods and fat rods (each representing 22%) (Fig. 7). During M and PM, short rods were the major targets of viruses, representing 32% and 31%, respectively. Cocci were the next target group after rods being 15%, 25% and 17% of the infected cells during PRM, M and PM, respectively. Filamentous forms represented the smallest fraction of virally infected cells consistently in all the seasons (9%, 2% and 5% during PRM, M and PM, respectively).

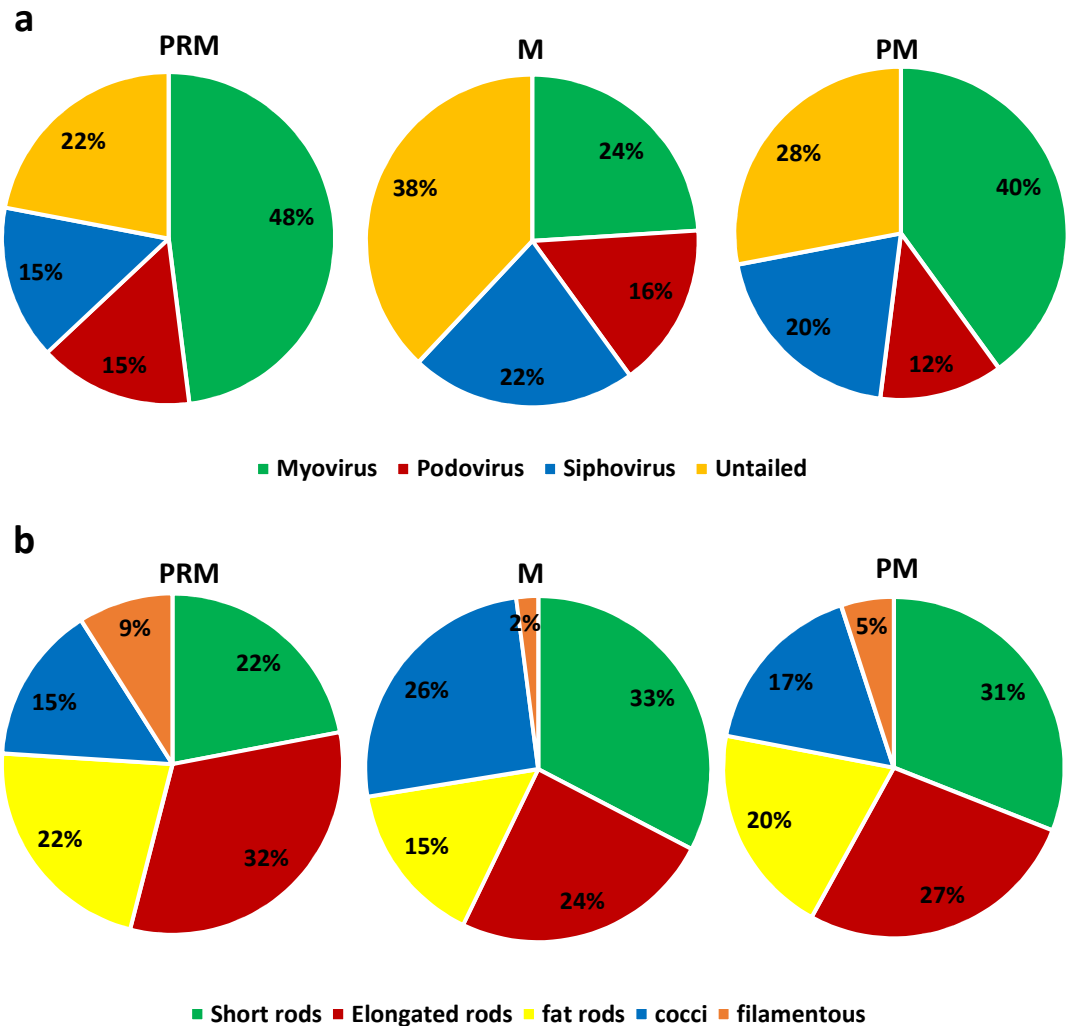

Fig. 7 Seasonal variations in (a) viral morphotypes and (b) infected prokaryotic morphotypes in the study region. PRM: pre-monsoon; M: monsoon; PM: post-monsoon

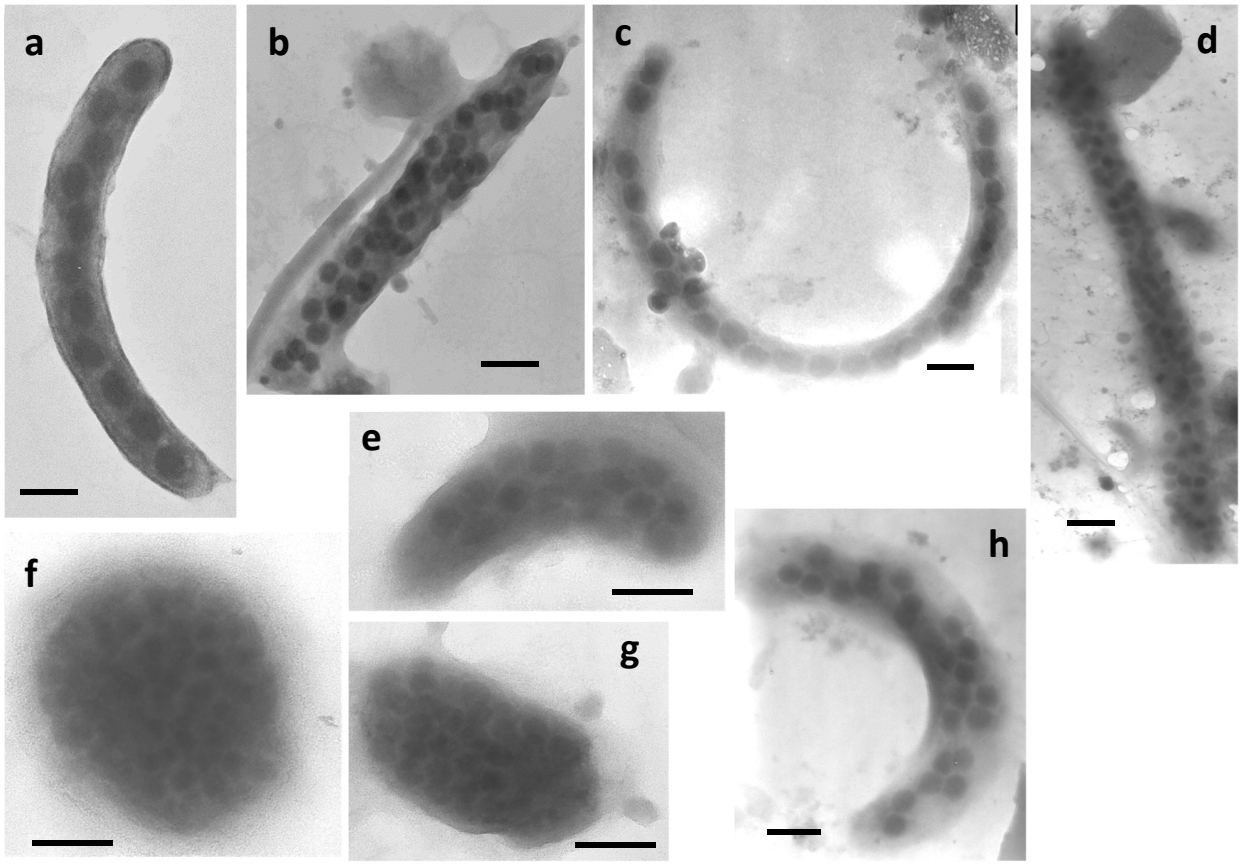

Fig. 8 Viral infected prokaryotic morphotypes in the collected water sample. (a, b, h) long rods, (c, d) filamentous, (f) coccus, (e) short rod and (g) fat rod. Scale bar = 100 nm

Viral burst sizes varied among different prokaryotic morphotypes with filamentous forms having the highest average burst size (81), followed by elongated rods (42), fat rods (36), cocci (30) and short rods (25) (Online Resource 2). Burst sizes of filamentous cells varied greatly with values ranging from 39-122. During PRM, the major fraction of virally infected prokaryotic morphotypes were elongated rods. Percentage of infected filamentous cells were also highest during PRM when compared to the other two seasons (9%, BS: 81). The PCA analysis performed for the two years presents an overview of the seasonal and spatial distribution patterns of VA and PA in relation to other environmental parameters. A clear distinction between the seasonal patterns of different biotic and abiotic variables are obvious in the PCA biplot (Fig. 9). PCA clearly demonstrates that the host abundance (Prokaryotic abundance and Chl *a*) is the major factor influencing the viral abundance and distribution, followed by temperature, salinity and dissolved oxygen. The PC1 axis effectively separated the sampling stations according to the seasonal variation.

343 Factor 1 (PC1) explained 42.63% of the total data variability and was positively correlated with salinity, Chl *a* and
344 inorganic nutrients, but negatively correlated with temperature and dissolved oxygen. Factor 2 (PC2) explained
345 32.83% of total data variability and was positively correlated with DO and chlorophyll a in 2014. In 2015, Factor 1
346 (PC1) explained 60.82% of the total data variability and Factor 2 (PC2) explained 18.30% of total data variability.
347 The nature of correlation parameters with physico-chemical parameters in 2015 were similar to 2014. The inter-
348 relationship of various physico-chemical and biological variables during PRM, M and PM was visualized in distance
349 based redundancy analysis (dbRDA) biplots (Fig 10), highlighting the strong correlations between VA and PA, and
350 the weak correlations with PO_4, SiO_4 and NH_4 in both 2014 and 2015
351
352

353

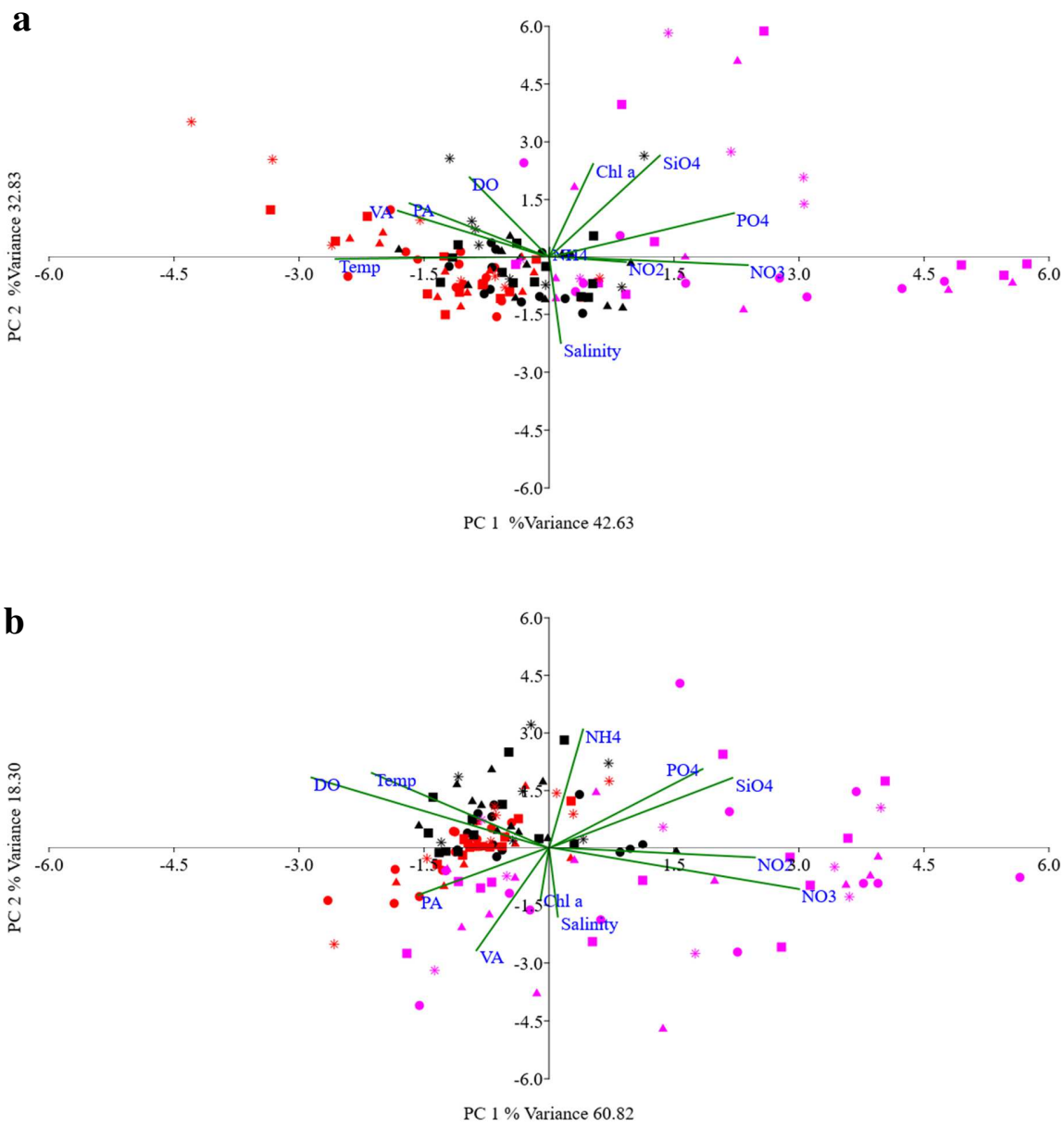

Fig. 9 Principal component analysis (PCA) representing the inter-relationship between various biological and physico-chemical parameters during (a) 2014 and (b) 2015. Observations during pre- monsoon (PRM, red), monsoon (M, pink) and post monsoon (PM, black) from stations, S1 (round), S2 (triangle), S3 (square) and S4 (star). Abbreviations: viral abundance (VA), prokaryotic abundance (PA), chlorophyll *a* (Chl *a*), temperature (Temp), dissolved oxygen (DO), nitrate (NO_3), nitrite (NO_2), ammonium (NH_4), phosphate (PO_4) and silicate (SiO_4)

354

355

a

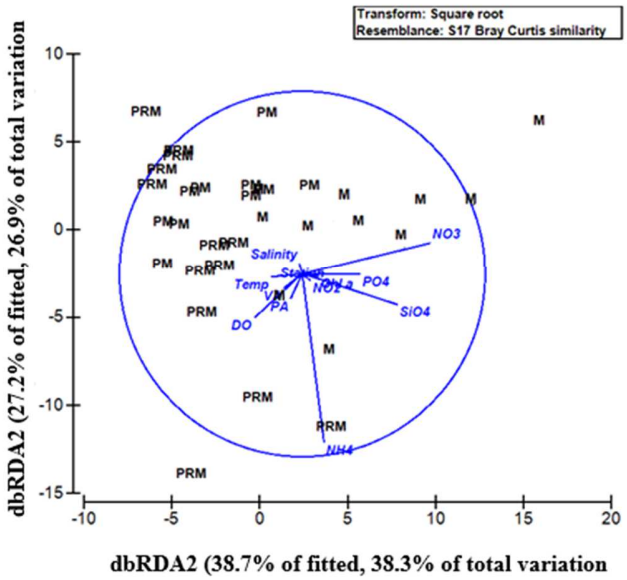

b

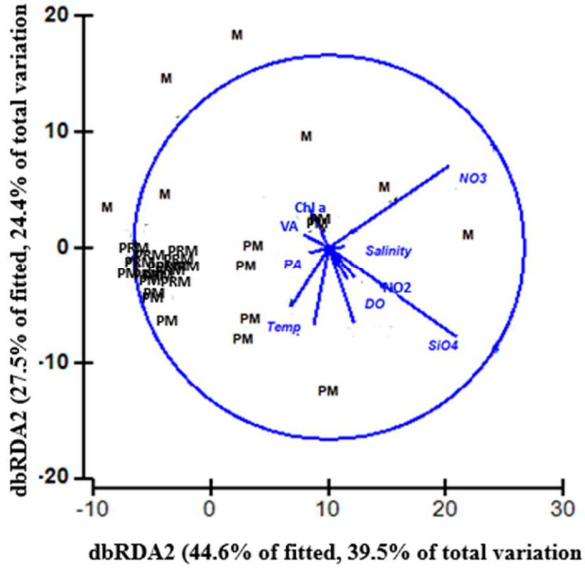

Fig. 10 Distance based linear model (DistLM) or distance based redundancy analysis (dbRDA) showing the inter-relationship of various physico-chemical and biological variables during pre monsoon (PRM), monsoon (M) and post monsoon (PM) in (a) 2014 and (b) 2015. Abbreviations: viral abundance (VA), prokaryotic abundance (PA), chlorophyll *a* (Chl *a*), dissolved oxygen (DO), nitrate (NO_3), nitrite (NO_2), ammonium (NH_4), phosphate (PO_4) and silicate (SiO_4)

Discussion

The present study represents the first description of the influence of seasonality on viral mediated processes in the eastern Arabian Sea (India). The data sets acquired from two consecutive years confirm the existence of a seasonal pattern for most of the studied environmental (biotic and abiotic) variables. A clear seasonality in terms of hydrography prevailed in the studied region. The water column was characterized by high temperature and salinity (Online Resource 3) but with low DO and nutrient concentrations during PRM. During monsoon period (June-Sep), coastal upwelling which brings nutrient rich waters towards the coast. In addition, there are strong cyclonic eddies in the sub-surface waters over the SE Arabian Sea during monsoon (Rao et al., 2008). In the present study, prominent upwelling features like surfacing of cool, less-oxygenated subsurface water mass towards the coast was evident during monsoon. The estuarine and freshwater influx was more in the coastal stations (S3 and S4), which plays a significant role in the distribution of plankton and prokaryotic community. The southwest monsoon period (M) was hence characterized by high nutrient concentrations of NO_3, PO_4 and SiO_4. The N:P ratios were comparatively high during M than PRM and PM. Nutrient enrichment favours the growth of phytoplankton and bacteria, which in turn supports the viral proliferation. A recent study by Sabbagh et al. (2020) reported that heterotrophic bacterial abundance is controlled by viruses throughout the year in the Red Sea as evident from the negative correlation between bacterial and viral abundances and positive correlation between bacterial mortality rates and viral abundance. Apart from the indirect effect of nutrient enrichment (such as increased host abundance and metabolism), a number of studies have reported on direct influence of nutrient concentrations, especially, phosphate and nitrate (which positively influence viral nucleic acid and protein syntheses), on viral abundance and viral production (Maat et al. 2014; Motegi et al. 2015).

The abundance of viruses and prokaryotes obtained from this study are comparable to other tropical oceanic regions (Winter et al. 2008; Gainer et al. 2017; Lara et al. 2017). Significant seasonal and spatial variations in the abundance of viruses and prokaryotes were explained from their interaction with various biotic and abiotic components of the system. The dbRDA biplot indicated that prokaryotic abundance was the most important predictor of viral abundance similar to reports from diverse oceanic regions (Middelboe 2000; Taylor et al. 2003; Parsons et al. 2012; Parvathi et al. 2015; De Corte et al. 2016). Another important determinant of viral abundance was temperature. An Artificial Neural Network-based model by Winter et al. (2012) has predicted temperature as the major factor determining prokaryotic and viral abundances. Seasonal variations in environmental parameters,

406 especially temperature and salinity, have been reported to affect the dynamics of host community structure (Suh et
407 al. 2015). Temperature have been reported as one of the key factors influencing variation in viral and prokaryotic
408 distribution and their interactions over broad spatial and temporal scales (Finke et al. 2017). Increasing temperature
409 was shown to increase bacterial respiration and bacterial production with adequate nutrient supply (Sarmento et al.
410 2010). The coupling between bacteria and phytoplankton enhanced with an increase in temperature by 2-6°C
411 (Hoppe et al. 2008). The carbon demand by bacteria also increase by ≈ 20% with increase in temperature without
412 any effect on their growth efficiency (Vazquez-Dominguez et al. 2007). Increase in viral abundance could also be
413 due to switching over of viruses from lytic from lysogenic mode under favorable temperatures (Williamson and Paul
414 2006). A decrease in latent period, increase in burst size and an increase in viral infectivity were observed with
415 increasing temperature in *Micromonas* viral populations (Maat et al. 2017). In our study, temperature may have
416 affected viral proliferation and activities directly or indirectly by controlling their host abundance and metabolism.
417 Viral-mediated processes such as host mortality and viral production followed the same seasonal pattern as that
418 of VA and PA with highest values in PRM (Online Resource 4). The existence of a strong and robust relationship
419 between viral production and both viral and prokaryote abundance has been reported from many marine regions
420 (Rowe et al. 2008). Several studies have demonstrated that increasing temperature had a positive influence on host
421 growth rate and subsequently resulted in increased viral production rates (Williamson and Paul 2006; Rowe et al.
422 2012; Demory et al. 2017). Viral induced mortality of prokaryote and phytoplankton hosts in the present study were
423 greatly influenced by viral production and temperature. Viral mediated mortality of phytoplankton communities has
424 been reported to increase at lower latitudes when compared to higher latitudes where grazer mediated mortality
425 predominated. This shift was associated with an increase in temperature and salinity at lower latitudes (Mojica et al.
426 2016). Viral lysis has been recognized as a significant means of mortality to the phytoplankton *Phaeocystis globosa*
427 in the North Sea. Viral lysis accounted for 5-66% of the total mortality of *P. globosa* during blooms (Baudoux et al.
428 2006). Viruses were also found to cause significant mortality to specific picophytoplankton groups in various coastal
429 and oligotrophic marine habitats (Baudoux et al. 2007; Baudoux et al. 2008). In the oligotrophic northeastern
430 Atlantic, viral lysis accounted for the release of 21% of the total carbon produced by picophytoplankton. In the
431 present study, viral lysis accounted for 7.98–28.9% of phytoplankton mortality with highest rates during PRM. High
432 viral production and turnover rates during PRM have been backed by the high burst sizes (42) of elongated rods.

High burst sizes along with higher host densities might have possibly contributed to the high infection frequencies and the increased host mortality during this season.

In this study, we evaluated viral morphological characteristics (viral morphotype), and virus-host interactions (infection pattern of viruses on different bacterial morphotypes) using a transmission electron microscopy (TEM) method during three seasons. Myoviridae was the dominant group in both PRM and PM, followed by untailed viruses. However, during monsoon untailed viruses were the most dominant viral morphotype. Myoviridae form the most dominant group in most marine environments as most viruses are phages, the viruses that infect bacteria (Wommack and Colwell 2000). Myoviruses have a broader host range than other phages, and are capable of infecting different species of bacteria. Few studies have also reported high abundance of non-tailed viruses (Auguet et al. 2006; Stopar et al. 2003; Bratbak et al. 1990). Various environmental parameters such as temperature influences the viral morphological characteristics of myoviridae, and temperature and salinity for untailed viruses and podoviridae (Brum et al. 2013). Several studies suggest that morphological characteristics are linked with seasons and environmental factors are important points to consider when assessing viral persistence (Espinosa et al. 2009). Based on TARA Ocean expedition, myovirus tails were longer in the Arabian Sea than Mediterranean Sea, Red Sea and Atlantic Ocean and capsid diameters of viruses were significantly larger in the Arabain Sea than those in the Indian, Atlantic and Pacific Oceans (Brum et al. 2013). The current study indicates that among different bacterial morphotypes (short rods, elongated rods, fat rods and cocci) rods were the most dominant forms representing about ~75% of the entire bacterial community throughout the study period and were more susceptible to viral infection. When compared to other morphotypes, the elongated rods had highest burst size (42 viruses bacterium^{-1}) probably due to the larger surface area of rods compared to other morphotypes. The present study should guide future work towards understanding the functional roles of the viruses in the southeastern Arabian Sea.

Conclusion

A clear seasonality in viral abundance and various viral processes in the southeastern Arabian Sea is apparent from the present study. Our observations on the seasonal drivers of viral dynamics were similar to those predicted for other oceanic regions such as the North Pacific and the Arctic Ocean. The seasonal variations in host abundance and temperature were the major driving factors of viral processes in the study region. Viral lysis is a significant means of host mortality in the coastal waters of the Arabian Sea especially during premonsoon season. By causing significant

460 percentage of host mortality, viruses may greatly contribute to the dissolved organic matter (DOM) pool. The
461 elevated viral activities during PRM indicated the highly active microbial loop in the oligotrophic premonsoon
462 season. Viral activities along with temperature play crucial role in controlling the host abundance and shaping the
463 host community structure in the Arabian Sea.

464 **Ackknowledgement**

465 The authors are thankful to the Director, CSIR-NIO, Goa, India and the Scientist-in-Charge, NIO (RC), Cochin,
466 India for their support and advice. The authors are grateful to Dr. Jyothibabu R. for helping with sample collection.

467 **Funding**

468 This work was supported by Indian National Centre for Ocean Information Services through grant-in-aid project
469 [NIO GAP 2807]. AS is grateful to University Grants Commission (UGC), New Delhi, India for her senior research
470 fellowship grant. JV is grateful to Council of Scientific and Industrial Research (CSIR), New Delhi, for her senior
471 research fellowship grant.

472 **Availability of data and material**

473 The datasets generated during and/or analysed during the current study are available from the corresponding author
474 on reasonable request.

475 Compliance with ethical standards

476 **Conflict of interest**

477 The authors declare that they have no conflict of interest.

478 **Ethics approval**

479 Not applicable

480 **Consent to participate**

481 All authors give their consent to participate in this publication.

482 **Consent for publication**

483 All authors agree with the content and give consent to publish this manuscript.

Code availability

Not applicable

References

Auguet JC, Montanie H, Lebaron P (2006) Structure of virioplankton in the Charente Estuary (France): transmission electron microscopy versus pulsed field gel electrophoresis. Microb ecol 51:197-208

Baudoux AC, Noordeloos AA, Veldhuis MJ, Brussaard CP (2006) Virally induced mortality of Phaeocystis globosa during two spring blooms in temperate coastal waters. Aquat Microb Ecol 44:207-217

Baudoux AC, Veldhuis MJ, Witte HJ, Brussaard CP (2007) Viruses as mortality agents of picophytoplankton in the deep chlorophyll maximum layer during IRONAGES III. Limnol Oceanogr 52:2519-29

Baudoux AC, Veldhuis MJ, Noordeloos AA, Van Noort G, Brussaard CP (2008) Estimates of virus-vs. grazing induced mortality of picophytoplankton in the North Sea during summer. Aquat Microb Ecol 52:69-82

Binder B (1999) Reconsidering the relationship between virally induced bacterial mortality and frequency of infected cells. Aquat Microb Ecol 18:207-215

Borrel G, Colombe J, Robin A, Lehours AC, Prangishvili D, Sime-Ngando T (2012) Unexpected and novel putative viruses in the sediments of a deep-dark permanently anoxic freshwater habitat. ISME J 6:2119

Bratbak G, Heldal M, Norland S, Thingstad TF (1990) Viruses as partners in spring bloom microbial trophodynamics. Appl Environ Microbiol 56:1400-1405

Breitbart M, Bonnain C, Malki K, Sawaya NA (2018) Phage puppet masters of the marine microbial realm. Nat Microbiol 3:754

Brum JR, Schenck RO, Sullivan MB (2013) Global morphological analysis of marine viruses shows minimal regional variation and dominance of non-tailed viruses. The ISME J 7:1738-1751

Burkill PH, Mantoura RF, Owens NJ (1993) Biogeochemical cycling in the northwestern Indian Ocean: a brief overview. Deep Sea Res Part II Top Stud Oceanogr 40:643-649

Calleja ML, Al-Otaibi N, Morán XA (2019) Dissolved organic carbon contribution to oxygen respiration in the central Red Sea. Sci Rep 9: https://doi.org/10.1038/s41598-019-40753-w

509 Campbell L, Landry MR, Constantinou J, Nolla HA, Brown SL, Liu H, Caron DA (1998) Response of microbial
510 community structure to environmental forcing in the Arabian Sea. Deep Sea Res Part II Top Stud
511 Oceanogr 45:2301-2325
512 Clokie MR, Millard AD, Mehta JY, Mann NH (2006) Virus isolation studies suggest short-term variations in
513 abundance in natural cyanophage populations of the Indian Ocean. J Mar Biolog Assoc UK 86:499-505
514 Cram JA, Parada AE, Fuhrman JA (2016) Dilution reveals how viral lysis and grazing shape microbial communities.
515 Limnol Oceanogr 61:889-905
516 De Corte D, Sintes E, Yokokawa T, Lekunberri I, Herndl GJ (2016) Large-scale distribution of microbial and viral
517 populations in the South Atlantic Ocean. Environ Microbiol Rep 8:305-315
518 Demory D, Arsenieff L, Simon N, Six C, Rigaut-Jalabert F, Marie D et al (2017). Temperature is a key factor in
519 Micromonas–virus interactions. ISME J 11:601
520 Ducklow HW (1993) Bacterioplankton distributions and production in the northwestern Indian Ocean and Gulf of
521 Oman, September 1986. Deep Sea Res Part II Top Stud Oceanogr 40:753-771
522 Evans C, Archer SD, Jacquet S, Wilson WH (2003) Direct estimates of the contribution of viral lysis and
523 microzooplankton grazing to the decline of a Micromonas spp. population. Aquat Microb Ecol 30:207-219
524 Finke J, Hunt B, Winter C, Carmack E, Suttle C (2017) Nutrients and other environmental factors influence virus
525 abundances across oxic and hypoxic marine environments. Viruses 9:152
526 Gainer PJ, Pound HL, Larkin AA, LeCleir GR, DeBruyn JM, Zinser ER, Johnson ZI, Wilhelm SW (2017)
527 Contrasting seasonal drivers of virus abundance and production in the North Pacific Ocean. PloS
528 One 12:e0184371
529 Gerson VJ, Madhu NV, Jyothibabu R, Balachandran KK, Nair M, Revichandran C (2014) Oscillating environmental
530 responses of the eastern Arabian Sea. Indian J Mar Sci 43:67-75
531 Grasshoff K, Ehrhardt MKK (1983) Methods of Seawater Analysis. Verlag Chemie, Weinheim, Germany
532 Hammer O, Harper DA, Ryan PD (2001) PAST: paleontological statistics software package for education and data
533 analysis. Palaeontol Electron 4:9
534 Hoppe HG, Breithaupt P, Walther K, Koppe R, Bleck S, Sommer U, Jürgens K (2008) Climate warming in winter
535 affects the coupling between phytoplankton and bacteria during the spring bloom: a mesocosm study. Aquat
536 Microb Ecol 51:105-115

537 Jain A, Bandekar M, Gomes J, Shenoy D, Meena RM, Naik H, Khandeparkar R, Ramaiah N (2014) Temporally
538 invariable bacterial community structure in the Arabian Sea oxygen minimum zone. Aquat Microb Ecol 73:51-
539 67
540 Jasna V, Parvathi A, Ram ASP, Balachandran KK, Madhu NV, Nair M, Jyothibabu R, Jayalakshmi KV,
541 Revichandran C, Sime-Ngando T (2017) Viral-induced mortality of prokaryotes in a tropical monsoonal
542 estuary. Front Microbiol 8:895
543 Jasna V, Parvathi A, Aswathy VK, Aparna S, Dayana M, Aswathy AJ, Madhu NV (2019) Factors determining
544 variations in viral abundance and viral production in a tropical estuary influenced by monsoonal cycles. Reg
545 Stud Mar Sci 1; https://doi.org/10.1016/j.rsma.2019.100589
546 Kumar SP, Prasad TG (1996) Winter cooling in the northern Arabian Sea. Curr Sci 71:834-841
547 Kumar SP, Madhupratap M, Kumar MD, Gauns M, Muraleedharan PM, Sarma VV, De Souza SN (2000) Physical
548 control of primary productivity on a seasonal scale in central and eastern Arabian Sea. J Earth Syst Sci
549 109:433-441
550 Lara E, Vaqué D, Sà EL, Boras JA, Gomes A, Borrull E et al (2017) Unveiling the role and life strategies of viruses
551 from the surface to the dark ocean. Sci Adv 3:e1602565
552 Maat DS, Crawfurd KJ, Timmermans KR, Brussaard CP (2014) Elevated CO2 and phosphate limitation favor
553 Micromonas pusilla through stimulated growth and reduced viral impact. Appl Environ Microbiol 80:3119-
554 3127
555 Maat D, Biggs T, Evans C, van Bleijswijk J, van der Wel N, Dutilh B, Brussaard C (2017) Characterization and
556 temperature dependence of Arctic Micromonas polaris viruses. Viruses 9:134
557 Mantoura RFC, Law CS, Owens NJP,,Burkhill PH, Woodward EMS,Howland RJM, Llewellyn CA (1993) Nitrogen
558 biogeochemical cycling in the northwestern Indian Deep Sea Res Part II Top Stud Oceanogr 40:651-671
559 McArdle BH, Anderson MJ (2001) Fitting multivariate models to community data: a comment on distance-based
560 redundancy analysis. Ecology 82:290-297
561 Middelboe M (2000) Bacterial growth rate and marine virus–host dynamics. Microb Ecol 40:114-124
562 Mojica KD, Brussaard CP (2014) Factors affecting virus dynamics and microbial host–virus interactions in marine
563 environments. FEMS Microbiol Ecol 89:495-515
564 Mojica KD, Huisman J, Wilhelm SW, Brussaard CP (2016) Latitudinal variation in virus-induced mortality of
565 phytoplankton across the North Atlantic Ocean. ISME J 10:500

566 Motegi C, Kaiser K, Benner R, Weinbauer MG (2014) Effect of P-limitation on prokaryotic and viral production in
567 surface waters of the Northwestern Mediterranean Sea. J Plankton Res 37:16-20
568 Naqvi SWA, Noronha RJ, Somasundar K, Gupta RS (1990) Seasonal changes in the denitrification regime of the
569 Arabian Sea. Deep Sea Res Part I Oceanogr Res Pap 37:593-611
570 Olson DB, Hitchcock GL, Fine RA, Warren BA (1993) Maintenance of the low-oxygen layer in the central Arabian
571 Sea. Deep Sea Res Part II Top Stud Oceanogr 40:673-685
572 Ortmann AC, Metzger RC, Liefer JD, Novoveska L (2011) Grazing and viral lysis vary for different components of
573 the microbial community across an estuarine gradient. Aquat microb ecol 65:143-157
574 Parsons TR, Maita Y, Lalli CM (1984) A Manual for Biological and Chemical Methods for Seawater Analysis.
575 Oxford, Pergamon
576 Parsons RJ, Breitbart M, Lomas MW, Carlson CA (2012) Ocean time-series reveals recurring seasonal patterns of
577 virioplankton dynamics in the northwestern Sargasso Sea. ISME J 6:273
578 Parvathi A, Jasna V, Jina S, Jayalakshmy KV, Lallu KR, Madhu NV, Muraleedharan KR, Naveen Kumar KR,
579 Balachandran KK (2015) Effects of hydrography on the distribution of bacteria and virus in Cochin estuary,
580 India. Ecol Res 30:85-92
581 Parvathi A, Jasna V, Aparna S, Ram ASP, Aswathy V, Balachandran KK, Muraleedharan KR, Mathew D, Sime-
582 Ngando T (2018) High Incidence of Lysogeny in the Oxygen Minimum Zones of the Arabian Sea (Southwest
583 Coast of India). Viruses 10:588
584 Patel A, Noble RT, Steele JA, Schwalbach MS, Hewson I, Fuhrman JA (2007) Virus and prokaryote enumeration
585 from planktonic aquatic environments by epifluorescence microscopy with SYBR Green I. Nat Protoc, 2:269
586 Pradeep Ram AS, Arnous B, Danger M, Carrias JF, Lacroix G, Sime-Ngando T (2010) High and differential viral
587 infection rates within bacterial 'morphopopulations' in a shallow sand pit lake (Lac de Créteil, France). FEMS
588 Microbiol Ecol 74:83-92
589 Ramaiah N, Raghukumar S, Gauns M (1996) Bacterial abundance and production in the central and eastern Arabian
590 Sea. Curr Sci 71:878-882
591 Ramaiah N, Fernandes V, Rodrigues VV, Paul JT, Gauns M (2009) Bacterioplankton abundance and production in
592 Indian Ocean Regions. Indian Ocean biogeochemical processes and ecological variability 1:119-132
593 Rao AD, Joshi M, Ravichandran M (2008) Oceanic upwelling and downwelling processes in waters off the west
594 coast of India. Ocean Dyn 58:213-226

595 Rodriguez F, Fernandez E, Head RN, Harbour DS, Bratbak G, Heldal M, Harris RP (2000) Temporal variability of
596 viruses, bacteria, phytoplankton and zooplankton in the western English Channel off Plymouth. J Mar Biolog
597 Assoc UK 80:575-586
598 Rowe JM, Saxton MA, Cottrell MT, DeBruyn JM, Berg GM, Kirchman DL, Hutchins DA, Wilhelm SW (2008)
599 Constraints on viral production in the Sargasso Sea and North Atlantic. Aquat Microb Ecol 52:233-244
600 Rowe JM, DeBruyn JM, Poorvin L, LeCleir GR, Johnson ZI, Zinser ER, Wilhelm SW (2012) Viral and bacterial
601 abundance and production in the Western Pacific Ocean and the relation to other oceanic realms. FEMS
602 Microbiol Ecol 79:359-370
603 Sabbagh EI, Huete-Stauffer TM, Calleja ML, Silva L, Viegas M, Morán XA (2020) Weekly variations of viruses and
604 heterotrophic nanoflagellates and their potential impact on bacterioplankton in shallow waters of the central Red
605 Sea. FEMS microbiol ecol 96: https://doi.org/10.1093/femsec/fiaa033
606 Sarmento H, Montoya JM, Vázquez-Domínguez E, Vaqué D, Gasol JM (2010) Warming effects on marine microbial
607 food web processes: how far can we go when it comes to predictions? Philos Trans R Soc Lond B, Biol
608 Sci 365:2137-2149
609 Shelford EJ, Middelboe M, Møller EF, Suttle CA (2012) Virus-driven nitrogen cycling enhances phytoplankton
610 growth. Aquat Microb Ecol 66:41-46
611 Stopar D, Černe A, Žigman M, Poljšak-Prijatelj M, Turk V (2003) Viral abundance and a high proportion of
612 lysogens suggest that viruses are important members of the microbial community in the Gulf of Trieste. Microb
613 ecol 46:249-256
614 Suh SS, Park M, Hwang J, Kil EJ, Jung SW, Lee S, Lee TK (2015) Seasonal dynamics of marine microbial
615 community in the South Sea of Korea. PLoS One 10:e0131633
616 Taylor GT, Hein C, Iabichella M (2003) Temporal variations in viral distributions in the anoxic Cariaco Basin. Aquat
617 Microb Ecol 30:103-116
618 Thomas R, Berdjeb L, Sime-Ngando T, Jacquet S (2011) Viral abundance, production, decay rates and life strategies
619 (lysogeny versus lysis) in Lake Bourget (France). Environ Microbiol 13:616-630
620 Vazquez-Dominiguez E, Vaque D, Gasol JM (2007) Ocean warming enhances respiration and carbon demand of
621 coastal microbial plankton. Glob Chang Biol 13:1327-1334

622 Weinbauer MG, Winter C, Höfle MG (2002) Reconsidering transmission electron microscopy based estimates of
623 viral infection of bacterio-plankton using conversion factors derived from natural communities. Aquat Microb
624 Ecol 27:103-110
625 Weinbauer MG, Bonilla-Findji O, Chan AM, Dolan JR, Short SM, Šimek K, Wilhelm SW, Suttle CA (2011)
626 Synechococcus growth in the ocean may depend on the lysis of heterotrophic bacteria. J Plankton Res 33:1465-
627 1476
628 Wiebinga CJ, Veldhuis MJ, De Baar HJ (1997) Abundance and productivity of bacterioplankton in relation to
629 seasonal upwelling in the northwest Indian Ocean. Deep Sea Res Part I Oceanogr Res Pap 44:451-476
630 Wilhelm SW, Brigden SM, Suttle CA (2002) A dilution technique for the direct measurement of viral production: a
631 comparison in stratified and tidally mixed coastal waters. Microb Ecol 43:168-173
632 Williamson SJ, Paul JH (2006) Environmental factors that influence the transition from lysogenic to lytic existence in
633 the ϕHSIC/Listonella pelagia marine phage–host system. Microb Ecol 52:217-225
634 Winter C, Moeseneder MM, Herndl GJ, Weinbauer MG (2008) Relationship of geographic distance, depth,
635 temperature, and viruses with prokaryotic communities in the eastern tropical Atlantic Ocean. Microb
636 Ecol 56:383-389
637 Winter C, Payet JP, Suttle CA (2012) Modeling the Winter–to–Summer Transition of Prokaryotic and Viral
638 Abundance in the Arctic Ocean. PloS one. 7:e52794
639 Wommack KE, Colwell RR (2000) Virioplankton: viruses in aquatic ecosystems. Microbiol Mol Biol Rev 64:69-114
640 Yang Y, Motegi C, Yokokawa T, Nagata T (2010) Large-scale distribution patterns of virioplankton in the upper
641 ocean. Aquat Microb Ecol 60:233-246
642
643
644
645
646
647

Table 1 F values based on three way ANOVA performed for various biotic and abiotic variables in the four stations (S1, S2, S3 and S4) during the three seasons (PRM, M and PM) of 2014 and 2015

	Variables	Year	Season	Station	Year × Season	Year × Station	Season × Station	Year × Season × Station
df		1	2	10	2	10	20	20
	VA	**25.246****	**8.667****	**2.020***	**5.544****	0.615	0.442	0.346
	PA	0.169	**18.406****	**3.154****	0.206	0.712	0.765	0.755
	DO	**18.192****	**27.056****	**5.826****	**7.433****	0.788	**2.009****	0.760
	NO_2	0.945	0.888	0.899	0.903	0.898	0.918	0.917
	NO_3	1.038	**60.656****	**3.274****	0.407	0.777	**3.301****	0.655
	NH_4	**14.098****	1.300	1.315	2.168	1.312	0.869	0.658
	SiO_4	**11.173****	**19.990****	**2.673****	1.937	0.279	0.563	0.336
	PO_4	**69.661****	**34.948****	1.851	**33.605****	0.204	0.374	0.246
	Chl *a*	1.043	**11.902****	**2.414****	0.282	0.778	2.004	0.726
	Temperature	0.351	**293.285****	**7.193****	**3.960***	0.966	1.045	0.159
	Salinity	2.743	0.769	**5.075****	**4.067***	1.156	1.250	0.962

VA: viral abundance, PA: prokaryotic abundance, Chl a: chlorophyll *a*, DO: dissolved oxygen, NO_3: nitrate, NO_2: nitrite, NH_4: ammonium, PO_4: phosphate and SiO_4: silicate. Significant F values at $p<0.05$ and $p<0.001$ are represented with * and **, respectively

652

Table 2 Seasonal and vertical variations in physico-chemical and biological parameters at the four stations (S1-S4) in 2014

Season	Parameters		S1			S2			S3			S4	
	Depth (m)		0.5	15	30	0.5	11	22	0.5	7	14	0.5	6
PRM	VA (10^7 VLP/mL)		0.70±0.17	0.41±0.00	0.53±0.19	0.71±0.12	0.50±0.13	0.42±0.15	0.75±0.38	0.44±0.15	0.45±0.09	1.17±0.71	0.72±0.57
	PA (10^6 cells/mL)		0.91±0.41	0.53±0.18	0.78±0.46	1.00±0.57	0.86±0.60	0.55±0.24	1.06±0.74	0.93±0.90	1.02±0.74	1.55±1.25	1.03±0.86
	Chl a		0.36±0.35	0.37±0.17	0.51±0.16	0.79±0.68	0.44±0.41	1.10±0.62	0.62±0.20	0.52±0.31	0.68±0.40	2.04±2.15	1.81±2.18
	DO (mL L^{-1})		5.35±1.00	6.02±1.15	4.75±0.78	4.65±1.70	4.70±1.54	3.85±1.75	5.10±2.15	4.52±1.64	4.82±2.35	4.95±1.22	4.27±1.33
	Temperature (°C)		30.55±0.57	29.28±0.37	29.10±0.25	30.40±0.76	29.56±0.50	29.15±0.35	30.39±0.84	29.84±1.23	29.40±0.59	30.60±0.4	29.66±0.66
	Salinity (PSU)		34.07±0.26	34.32±0.15	34.73±0.60	34.05±0.10	34.2±0.05	34.56±0.32	33.83±0.25	34.23±0.46	33.56±0.74	32.67±2.13	33.24±2.49
	Nutrients(µ	NO_3	0.46±0.32	0.36±0.20	0.80±0.77	0.43±0.35	0.64±0.40	1.02±0.52	0.52±0.50	0.66±0.35	0.79±0.61	0.75±0.44	1.33±0.76
	mol L^{-1})	PO_4	0.30±0.11	0.35±0.16	0.33±0.38	0.59±0.57	0.62±0.65	0.62±0.70	0.50±0.14	0.3±0.18	0.45±0.37	0.69±0.38	0.72±0.42
M	VA (10^7 VLP/mL)		0.28±0.10	0.21±0.05	0.17±0.03	0.24±0.12	0.23±0.09	0.09±0.03	0.29±0.09	0.22±0.13	0.18±0.13	0.45±0.13	0.24±0.11
	PA (10^6 cells/mL)		0.55±0.12	0.37±0.00	0.39±0.19	0.39±0.09	0.39±0.03	0.26±0.15	0.53±0.08	0.33±0.12	0.31±0.09	0.57±0.13	0.32±0.13
	Chl a		1.50±2.23	0.76±0.61	0.65±0.75	9.34±13.53	0.98±0.76	1.03±1.11	11.42±16.7	0.84±0.85	1.08±0.90	1.86±0.91	2.33±1.24
	DO (mL L^{-1})		6.14±2.86	3.68±1.91	2.71±2.87	7.78±4.17	6.23±1.01	2.02±2.24	8.59±2.51	4.06±3.00	1.95±1.49	5.69±1.31	7.11±4.15
	Temperature (°C)		27.74±0.32	25.89±1.79	24.74±2.44	27.52±0.71	26.71±1.05	24.51±1.78	27.51±0.56	26.72±1.68	25.47±1.80	27.09±0.82	26.61±0.98
	Salinity (PSU)		29.83±7.23	34.78±0.59	35.16±0.32	31.57±3.62	34.80±0.38	35.22±0.33	29.53±6.83	33.84±1.55	34.56±0.87	31.52±3.64	28.16±11.50
	Nutrients(µ	NO_3	0.89±0.21	7.04±2.39	12.91±3.73	1.16±0.14	3.95±1.59	14.30±2.27	0.81±0.33	8.27±5.26	14.05±11.4	2.09±1.81	6.45±4.97
	mol L^{-1})	PO_4	1.27±0.69	1.68±0.85	1.90±0.84	1.47±1.29	1.37±0.74	1.93±1.27	1.71±1.53	1.83±1.52	2.27±1.63	2.2±1.66	1.54±1.00
PM	VA (10^7 VLP/mL)		0.31±0.15	0.19±0.11	0.20±0.17	0.40±0.26	0.22±0.19	0.12±0.05	0.35±0.22	0.31±0.18	0.19±0.08	0.50±0.11	0.26±0.09
	PA (10^6 cells/mL)		0.57±0.17	0.41±0.17	0.36±0.08	0.66±0.45	0.37±0.13	0.30±0.09	0.55±0.23	0.43±0.13	0.41±0.17	0.87±0.33	0.45±0.08
	Chl a		0.27±0.28	0.32±0.25	0.43±0.26	0.58±0.36	0.37±0.29	0.58±0.33	0.59±0.46	0.65±0.49	0.60±0.34	1.33±1.01	1.08±0.71
	DO (mL L^{-1})		7.44±1.44	6.59±2.11	5.26±2.01	6.77±1.26	5.76±2.43	4.97±1.75	6.75±1.10	5.76±1.3	5.38±1.39	7.72±3.27	5.73±1.53
	Temperature (°C)		29.06±0.44	28.81±0.31	28.27±0.41	29.27±0.45	28.71±0.39	28.57±0.26	29.53±0.61	28.9±0.31	28.61±0.31	29.57±0.89	28.90±0.88
	Salinity (PSU)		32.98±1.35	34.54±0.88	35.08±0.72	31.60±2.14	34.29±1.12	34.86±0.63	30.88±3.76	33.98±0.52	34.57±0.71	29.48±2.06	34.23±1.62
	Nutrients(µ	NO_3	1.45±1.23	1.00±0.46	1.07±0.55	1.00±1.12	1.73±1.30	1.43±0.60	1.79±1.86	1.43±1.11	1.14±0.61	2.40±1.18	1.50±1.00
	mol L^{-1})	PO_4	0.39±0.29	0.32±0.13	0.42±0.13	0.46±0.19	0.50±0.33	0.54±0.26	0.58±0.50	0.44±0.45	0.83±0.19	0.91±0.76	0.67±0.39

PRM: pre monsoon, M: monsoon, PM: post monsoon, VA: viral abundance, PA: prokaryotic abundance, DO: dissolved oxygen, NO_3: nitrate, PO_4: phosphate

655

656

657

658

659

660

661

Table 3 Seasonal and vertical variations in physico—chemical and biological parameters at the four stations (S1-S4) in 2015

Season	Parameters		S1			S2			S3			S4	
	Depth (m)		0.5	15	30	0.5	11	22	0.5	7	14	0.5	6
PRM	**VA (10^7 VLP/mL)**		1.47±0.65	0.65±0.39	0.59±0.90	0.92±0.42	0.50±0.44	0.54±0.33	0.89±0.38	0.76±0.91	0.65±0.24	1.12±1.29	0.70±0.63
	PA (10^6 cells/mL)		2.34±1.64	0.63±0.54	0.97±1.87	0.39±0.39	0.48±0.41	0.53±0.42	0.59±0.28	0.69±1.02	0.49±0.46	1.98±2.13	0.73±0.44
	Chl a		0.2±0.30	0.10±0.12	0.53±0.17	0.27±0.24	0.32±0.21	0.64±0.20	0.49±0.36	0.40±0.29	0.57±0.16	1.01±0.66	1.30±0.49
	DO (mL L^{-1})		7.05±0.19	6.92±0.34	6.77±0.82	6.98±0.56	6.69±0.39	6.29±1.08	6.39±0.25	6.39±0.25	6.05±0.26	6.14±0.53	5.59±1.04
	Temperature (°C)		30.37±0.78	29.87±0.68	29.4±0.46	30.49±0.62	30.08±0.69	29.54±0.54	30.47±0.39	29.88±0.60	29.81±0.58	31.10±0.82	30.44±0.38
	Salinity (PSU)		34.04±0.34	34.19±0.33	33.04±2.1	33.41±1.38	34.22±0.23	32.51±2.73	32.51±1.56	34.02±0.18	34.05±0.20	32.85±0.88	32.96±1.42
	Nutrients(µ mol L^{-1})	**NO_3**	2.07±1.08	1.19±0.24	1.23±0.57	1.44±0.50	1.21±0.26	2.56±0.76	2.00±1.08	1.78±1.52	1.36±0.72	1.80±0.58	2.34±0.75
		PO_4	0.23±0.10	0.36±0.23	0.28±0.15	0.20±0.03	0.33±0.30	0.32±0.24	0.50±0.23	0.41±0.28	0.37±0.09	0.79±0.43	0.79±0.60
M	**VA (10^7 VLP/mL)**		1.60±1.62	0.78±0.59	0.13±0.08	0.85±0.62	1.21±1.64	1.26±1.62	0.74±0.31	0.76±0.43	0.99±0.98	1.26±1.42	0.46±0.36
	PA (10^6 cells/mL)		0.78±0.98	0.39±0.46	0.10±0.16	0.28±0.38	0.33±0.30	0.30±0.18	0.61±0.66	0.53±0.37	0.39±0.29	0.76±0.77	0.39±0.43
	Chl a		1.97±1.23	1.75±0.88	0.69±0.53	2.07±1.89	2.55±0.75	2.34±1.02	1.83±1.21	4.13±0.85	2.82±1.22	2.98±1.35	2.29±0.88
	DO (mL L^{-1})		7.57±1.11	3.48±2.57	1.69±1.76	7.38±1.25	4.48±3.51	3.25±3.73	6.58±1.8	5.01±3.47	3.34±3.79	6.32±0.65	2.88±2.54
	Temperature (°C)		25.70±0.51	24.22±0.53	23.09±0.35	26.2±0.75	25.42±0.83	24.01±0.75	26.52±1.68	24.86±0.93	24.12±0.85	26.35±1.2	24.22±0.56
	Salinity (PSU)		34.73±0.46	34.81±0.56	34.88±1.23	33.94±5.81	34.48±1.35	34.90±4.68	29.18±8.60	34.84±0.53	30.66±0.73	32.78±7.3	34.58±2.06
	Nutrients(µ mol L^{-1})	**NO_3**	2.38±2.15	7.33±9.01	17.94±3.81	2.41±2.11	4.93±3.20	12.06±6.86	7.67±9.12	5.01±3.31	9.82±9.97	6.91±10.41	7.08±7.09
		PO_4	0.15±0.18	0.23±0.21	0.5±0.48	0.13±0.13	0.32±0.30	0.57±0.56	0.44±0.55	0.35±0.31	0.54±0.67	0.41±0.46	0.45±0.43
PM	**VA (10^7 VLP/mL)**		0.61±0.14	0.46±0.15	0.34±0.11	0.46±0.17	0.27±0.15	0.19±0.04	0.58±0.22	0.42±0.13	0.42±0.16	0.70±0.24	0.58±0.22
	PA (10^6 cells/mL)		0.28±0.21	0.23±0.14	0.16±0.17	0.28±0.31	0.17±0.16	0.16±0.16	0.75±0.20	0.55±0.23	0,52±0.12	0.76±0.10	0.58±0.06
	Chl a		0.33±0.44	0.27±0.36	0.29±0.08	0.78±0.98	0.54±0.07	0.37±0.16	0.55±0.45	0.63±0.02	0.43±0.24	0.97±0.07	1.21±0.96
	DO (mL L^{-1})		8.06±1.23	6.85±2.19	7.39±1.37	9.95±0.73	7.81±0.97	6.77±2.56	8.72±1.43	8.38±1.39	7.56±0.60	7.93±1.36	7.41±1.00
	Temperature (°C)		28.68±0.61	28.59±0.44	28.16±0.20	28.73±0.58	28.47±0.20	28.42±0.14	29.32±0.83	28.60±0.22	28.41±0.06	29.22±0.18	28.82±0.04
	Salinity (PSU)		32.73±2.05	34.80±0.83	34.94±1.01	32.78±2.04	34.59±0.39	34.81±0.71	30.14±6.04	34.17±0.25	34.75±0.57	29.92±4.94	33.86±0.14
	Nutrients(µ mol L^{-1})	**NO_3**	2.59±1.72	1.73±2.13	1.99±2.23	1.71±1.67	0.30±0.20	2.08±3.43	1.58±1.92	0.25±0.07	0.62±0.24	2.63±2.48	1.26±1.63
		PO_4	0.35±0.28	0.20±0.14	0.38±0.07	0.31±0.12	0.30±0.25	0.41±0.22	0.36±0.29	0.33±0,,15	0.4±0.31	0.49±0.31	0.38±0.30

PRM: pre monsoon, M: monsoon, PM: post monsoon, VA: viral abundance, PA: prokaryotic abundance, DO: dissolved oxygen, NO_3: nitrate and PO_4: phosphate

663

664 **Figure Legends**

665 **Fig 1** Sampling locations in the Arabian Sea. Water samples were collected from four stations of a transect
666 perpendicular to the coast of Kochi on monthly basis during 2014 and 2015. Sampling locations are marked as S1,
667 S2, S3 and S4

668 **Fig. 2** Variations in viral and prokaryotic abundance (VA & PA) during pre-monsoon (PRM, blue), monsoon (M,
669 red) and post-monsoon (PM, green) seasons. (a) VA in 2014, (b) VA in 2015, (c) PA in 2014 and (d) PA in 2015

670 **Fig. 3** Variations in (a) viral production (VP) and (b) viral turnover rates (VTR) at stations S1 and S4 during pre-
671 monsoon (PRM, blue), monsoon (M, red) and post-monsoon (PM, green) in 2014

672 **Fig. 4** Seasonal variations in (a) frequency of infected cells (FIC) and (b) viral induced prokaryotic mortality
673 (VIPM) at S1 and S4 in 2014. Pre-monsoon (PRM): blue; monsoon (M): red; post-monsoon (PM): green

674 **Fig. 5** Seasonal variations in viral mediated mortality (VMM) and microzooplankton grazing mortality (MGM) at
675 S1 and S4 in 2014. pre-monsoon (PRM): blue; monsoon (M): red; post-monsoon (PM): green

676 **Fig. 6** Viral morphotypes from the Arabian Sea (a, b, c, d) myoviruses, (e, f) non-tailed viruses and (g) siphoviruses.
677 Scale bar = 50 nm

678 **Fig. 7** Seasonal variations in (a) viral morphotypes and (b) infected prokaryotic morphotypes in the study region.
679 PRM: pre-monsoon; M: monsoon; PM: post-monsoon

680 **Fig. 8** Viral infected prokaryotic morphotypes in the collected water sample. (a, b, h) long rods, (c, d) filamentous,
681 (f) coccus, (e) short rod and (g) fat rod. Scale bar = 100 nm

682 **Fig. 9** Principal component analysis (PCA) representing the inter-relationship between various biological, physical
683 and chemical parameters during (a) 2014 and (b) 2015. Observations during pre-monsoon (PRM, red), monsoon (M,
684 pink) and post-monsoon (PM, black) from stations, S1 (round), S2 (triangle), S3 (square) and S4 (star).
685 Abbreviations: viral abundance (VA), prokaryotic abundance (PA), chlorophyll *a* (Chl *a*), temperature (Temp),
686 dissolved oxygen (DO), nitrate (NO_3), nitrite (NO_2), ammonium (NH_4), phosphate (PO_4) and silicate (SiO_4)

687 **Fig. 10** Distance based linear model (DistLM) showing the inter-relationship of various physical, chemical and
688 biological variables during pre-monsoon (PRM), monsoon (M) and post-monsoon (PM) in (a) 2014 and (b) 2015.
689 Abbreviations: viral abundance (VA), prokaryotic abundance (PA), chlorophyll *a* (Chl *a*), dissolved oxygen (DO),
690 nitrate (NO_3), nitrite (NO_2), ammonium (NH_4), phosphate (PO_4) and silicate (SiO_4)

691 **Online Resource 1** Variations in (a & b) temperature, (c & d) salinity and (e & f) Chl a at the four stations, S1-S4
692 during pre-monsoon (PRM, blue), monsoon (M, red) and post-monsoon (PM, green)

693 **Online Resource 2** Variations in the number of average progenies produced per infected cells (burst size) of
694 different prokaryotic morphotypes

695 **Online Resource 3** Vertical profiles of temperature and salinity illustrating the seasonal changes in hydrography. (a-
696 c) PRM (pre monsoon), M (monsoon) & PM (post monsoon) seasons in 2014, (d-f) PRM, M & PM seasons in 2015

697 **Online Resource 4** Principal component analysis (PCA) representing different biological, physical and chemical
698 factors influencing viral processes in the study region during 2014. Premonsoon (PRM, green), monsoon (M, black),
699 and post monsoon (PM, red). Abbreviations: viral abundance (VA), prokaryotic abundance (PA), viral production
700 (VP), viral turnover rate (VTR), frequency of visibly infected cells (FVIC), frequency of infected cells (FIC), viral
701 induced prokaryotic mortality (VIPM), viral mediated mortality of phytoplankton (VMM), microzooplankton
702 grazing mortality (MGM), chlorophyll *a* (Chl *a*), temperature (Temp), dissolved oxygen (DO), nitrate (NO_3), nitrite
703 (NO_2), ammonium (NH_4), phosphate (PO_4) and silicate (SiO_4)